



Article

H₂O₂-Responsive Hormonal Status Involves Oxidative Burst Signaling and Proline Metabolism in Rapeseed Leaves

Bok-Rye Lee ^{1,†} , Van Hien La ^{1,2,†}, Sang-Hyun Park ¹, Md Al Mamun ¹, Dong-Won Bae ³ and Tae-Hwan Kim ^{1,*}

¹ Department of Animal Science, Institute of Agricultural Science and Technology, College of Agriculture & Life Science, Chonnam National University, Gwangju 61186, Korea; turfphy@jnu.ac.kr (B.-R.L.); trungtamnccttubdkh@tuaf.edu.vn (V.H.L.); ghost1284@jnu.ac.kr (S.-H.P.); 187054@jnu.ac.kr (M.A.M.)

² Department of Biotechnology and Food Technology, Thai Nguyen University of Agriculture and Forestry, Thai Nguyen 24000, Vietnam

³ Central Instruments Facility, Gyeongsang National University, Jinju 52828, Korea; bdwon@gnu.ac.kr

* Correspondence: grassl@chonnam.ac.kr; Tel.: +82-62-530-2126

† These authors contributed equally to this work.

Abstract: Drought alters the level of endogenous reactive oxygen species (ROS) and hormonal status, which are both involved in the regulation of stress responses. To investigate the interplay between ROS and hormones in proline metabolism, rapeseed (*Brassica napus* L.) plants were exposed to drought or exogenous H₂O₂ (Exo-H₂O₂) treatment for 10 days. During the first 5 days, the enhanced H₂O₂ concentrations in drought treatment were associated with the activation of superoxide dismutase (SOD) and NADPH oxidase, with enhanced ABA and SA levels, while that in Exo-H₂O₂ treatment was mainly associated with SA-responsive POX. During the latter 5 days, ABA-dependent ROS accumulation was predominant with an upregulated oxidative signal-inducible gene (*OX11*) and *MAPK6*, leading to the activation of ABA synthesis and the signaling genes (*NCED3* and *MYC2*). During the first 5 days, the enhanced levels of P5C and proline were concomitant with SA-dependent *NDR1*-mediated signaling in both drought and Exo-H₂O₂ treatments. In the latter 5 days of drought treatment, a distinct enhancement in *P5CR* and *ProDH* expression led to higher proline accumulation compared to Exo-H₂O₂ treatment. These results indicate that SA-mediated P5C synthesis is highly activated under lower endogenous H₂O₂ levels, and ABA-mediated *OX11*-dependent proline accumulation mainly occurs with an increasing ROS level, leading to *ProDH* activation as a hypersensitive response to ROS and proline overproduction under severe stress.

Keywords: abscisic acid; *Brassica napus*; drought; hydrogen peroxide; proline; salicylic acid



Citation: Lee, B.-R.; La, V.H.; Park, S.-H.; Mamun, M.A.; Bae, D.-W.; Kim, T.-H. H₂O₂-Responsive Hormonal Status Involves Oxidative Burst Signaling and Proline Metabolism in Rapeseed Leaves. *Antioxidants* **2022**, *11*, 566. <https://doi.org/10.3390/antiox11030566>

Academic Editor: José Antonio Hernández Cortés

Received: 15 February 2022

Accepted: 14 March 2022

Published: 16 March 2022

Publisher's Note: MDPI stays neutral with regard to jurisdictional claims in published maps and institutional affiliations.



Copyright: © 2022 by the authors. Licensee MDPI, Basel, Switzerland. This article is an open access article distributed under the terms and conditions of the Creative Commons Attribution (CC BY) license (<https://creativecommons.org/licenses/by/4.0/>).

1. Introduction

Reactive oxygen species (ROS) are generated due to the univalent reduction of oxygen in the metabolic pathway as one of the earliest responses of plant cells to drought [1–6] and pathogen infection [7–9]. Excess of ROS causes oxidative stress that can damage proteins, lipids, and DNA [10–12]. ROS also function as secondary messengers in the regulation of stress responses in plants [13–15]. Thus, the steady-state level of ROS in cells needs to be tightly regulated by ROS-scavenging and ROS-producing proteins, such as peroxidases (POXs), NADPH oxidase, superoxide dismutase (SOD), and catalase (CAT) [16–18], as well as by non-enzymatic metabolic pathways (e.g., glutathione-ascorbate cycle) [19,20]. As the most stable among the ROS, H₂O₂ is appropriate to play this function [2,17,21]. H₂O₂ produced by cytosolic membrane-bound NADPH oxidase is the key player associated with the ROS-related signal transduction [14,20,21]. Oxidative burst-mediated signaling is required for the induction of the *oxidative signal-inducible gene* (*OX11*). The *OX11* encoding a serine/threonine kinase is induced in response to a wide range of H₂O₂-generating stimuli [13]. Activation of *OX11* results in the activation of a mitogen-activated protein kinase (MAPK) cascade (MAPK3/6) and the induction or activation of different transcription

factors that regulate the ROS-scavenging and ROS-producing pathways [2]. In addition, plants exposed to stress stimuli often upregulate ROS (especially H₂O₂) and phytohormone signaling [5,8,22]. In this regard, the interaction between H₂O₂ and hormones has been widely studied under different environmental stresses in various plants [6,20,23,24].

Another common response to drought stress is the accumulation of proline along with enhanced H₂O₂ levels. The H₂O₂ produced by NADPH oxidase increases proline accumulation to scavenge ROS [25–27], whereas overproduced proline leads to increase in endogenous ROS [28–30]. Numerous studies have shown that ROS and proline accumulation are regulated by stress-responsive hormones, of which the best studied are abscisic acid (ABA) and salicylic acid (SA). Drought, in general, increases levels of both endogenous ABA and SA, as well as their signaling along with an enhanced H₂O₂ level [5,6,31]. ROS (particularly H₂O₂) is thought to be a part of ABA signaling. For instance, drought-enhanced H₂O₂ from NADPH oxidase [27,32] induces proline accumulation via upregulation of pyrroline-5-carboxylate synthetase (P5CS) and downregulation of proline dehydrogenase (ProDH) [5,33] in an ABA-dependent manner [31,34]. Our previous studies have shown that severe drought symptoms, characterized by the ABA-responsive proline and H₂O₂ accumulation leading to the oxidized state of redox, are alleviated by a SA-mediated antagonistic depression of ABA responses [5,31]. Despite the increasing evidence of a close relationship between ROS and proline metabolism linked to hormonal interaction, the hormonal regulation of proline metabolism in relation to endogenous H₂O₂ levels and different H₂O₂ sources (e.g., drought-induced and exogenous H₂O₂), which are partially associated with the discrepancies observed in their regulatory roles in stress response and resistance processes, has rarely been studied.

In the present study, we hypothesized that (1) the regulatory actions of drought-induced H₂O₂ (as the internal H₂O₂ trigger) and of exogenous H₂O₂ are different in ROS signal transduction and (2) the altered H₂O₂ levels and their signaling modulate proline metabolism with hormonal interaction. To test these hypotheses, antioxidant activity, ABA and SA responses, and proline metabolism were interpreted with respect to the altered H₂O₂ levels and ROS signaling, in response to drought or exogenous-H₂O₂ treatment.

2. Materials and Methods

2.1. Plant Materials, Growth Conditions, and Stress Treatments

Plants of the rapeseed (*Brassica napus* L.) cultivar Capitol were used for this study (Gwangju, Korea) and cultivated as previously described by Lee. et al. [35]. The seedlings at four-leaf stage were transferred to soil-filled 2 L pots and irrigated continuously in complete nutrient solution for 6 weeks. Then, plants were divided into three groups according to morphological similarity. The first group was irrigated with 200 mL of water for the well-watered plants (control), the second with 20 mL of water (drought), and the third was daily foliar-sprayed with 20 mL of 50 µM H₂O₂ under well-watered conditions (exogenous-H₂O₂ (Exo-H₂O₂)) for 10 days. Sampling was performed at 0, 5, and 10 days after treatment. In this study, the mature leaves ranked 4–12 (i.e., rank 1 for the oldest leaf) were considered. After sampling, leaf tissues were cut and frozen immediately in liquid nitrogen and stored in a deep-freezer (−80 °C) until further analysis.

2.2. Measurement of Leaf Water Potential (Ψ_w) and Chlorophyll Content

For measurement of leaf water potential (Ψ_w), the seventh leaf was cut and then inserted the pressure chamber (PMS Instruments, Corvallis, OR, USA) to expose the cut end of the petiole on the outside. Afterwards, pressure was applied to the chamber until liquid was observed at the end of petiole, which corresponds to the Ψ_w . For total chlorophyll, approximately 100 mg of fresh-cut leaves were extracted with 10 mL of 99% dimethyl sulfoxide [36]. After 48 h, the absorbance of the supernatants was read at 645 and 663 nm and calculated using the following formula: total chlorophyll (µg/mL) = 20.2 A₆₄₅ + 8.02 A₆₆₃.

2.3. Determination of Phytohormones

For the quantification of phytohormones, 50 mg of finely ground fresh leaves was extracted with 500 μ L of the extraction solvent (2-propanol/H₂O/concentrated HCl (2:1:0.002, *v/v/v*)) containing d₆-ABA and d₆-SA as the internal standard (50 ng) for ABA and SA, respectively, for 24 h at 4 °C [37]. The supernatant was mixed with 1 mL of dichloromethane and at 13,000 \times *g* for 5 min at 4 °C. After centrifugation, two phases were formed. The supernatant in the lower phase was transferred to clean screw-cap glass vial and dried using a nitrogen evaporator with nitrogen flow. Then, samples were re-suspended in 1 mL of methanol and further purified with filtering through 0.22 μ m organic membrane filters. The extracted solution transferred to vials with a glass insert and stored at –80 °C until high-performance liquid chromatography electrospray ionization tandem mass spectrometry (HPLC-ESI-MS/MS) analysis. Ten microliters of plant extracts were injected onto an Agilent 1100 HPLC system, equipped with a Waters C18 column (150 \times 2.1 mm, 5 μ m) and API3000 MS-MRM (Applied Biosystems, Waltham, MA, USA).

2.4. Antioxidant Enzyme Activities

For extraction of antioxidant enzymes, approximately 500 mg of finely ground fresh samples were extracted with 1.5 mL of 100 mM potassium phosphate buffer pH 7.5 containing 2 mM phenylmethylsulfonyl fluoride. After centrifugation at 14,000 \times *g* for 20 min at 4 °C, the supernatants were used as enzyme sources [38]. Protein concentration was determined using Bradford reagent with bovine serum albumin as a proteins standard. For cell wall POX activity, the oxidation of guaiacol was evaluated by monitoring the increase in absorbance at 470 nm for 1 min (coefficient of absorbance, $\epsilon = 26.6 \text{ mM}^{-1} \text{ cm}^{-1}$) [39]. One unit of enzyme activity was defined as the amount of enzyme causing the formation of 1 M tetraguaiacol per min. SOD activity was measured by its ability to inhibit the photoreduction of nitroblue tetrazolium (NBT) [11]. One unit of enzyme activity was defined as the amount of enzyme causing 50% inhibition of NBT photoreduction in comparison with tubes lacking the plant extract. CAT activity was monitored by following the decrease in absorbance at 240 nm due to H₂O₂ consumption ($\epsilon = 36 \text{ mM}^{-1} \text{ cm}^{-1}$). One unit of enzyme activity was defined as the amount of enzyme causing the degradation of 1 μ mol of H₂O₂ per min [38].

2.5. Chemical Analysis

Fresh samples (0.5 g) were mixed with 1.5 mL of 50 mM KPO₄[–] buffer (pH 7.0) and centrifuged at 10,000 \times *g* for 25 min at 4 °C. After centrifugation, the supernatants were used to determine the superoxide anion radical (O₂^{•–}) and H₂O₂ concentration. The O₂^{•–} concentration was conducted according to the method of Lee et al. [11] by O₂^{•–} oxidation of hydroxylamine. Briefly, the supernatants were mixed with hydroxylamine solution, incubated for 1 h at 25 °C, and then reacted with 17 mM sulfanilic acid and 7 mM *o*-naphthylamine for 20 min. The absorbance was read at 530 nm and calculated using the NO₂ standard. The H₂O₂ concentration was measured by the method of Lin and Kao [40]. The supernatants were mixed with 0.1% titanium chloride in 20% H₂O₂. The absorbance was immediately read at 410 nm. The H₂O₂ concentration was determined by measuring the absorbance at 410 nm and calculated using the extinction coefficient of 0.28 $\text{mM}^{-1} \text{ cm}^{-1}$. The lipid peroxidation level was determined by measuring the concentration of malondialdehyde (MDA), as described previously [3]. Fresh samples (0.5 g) were extracted with 0.1% trichloroacetic acid, centrifuged, mixed with 0.5% tributuric acid in 20% TCA, and then boiled for 30 min at 95 °C. The absorbance was measured at 532 nm and calculated using the extinction coefficient of 155 $\text{mM}^{-1} \text{ cm}^{-1}$. The concentration of proline and pyrroline-5-carboxylate (P5C) was measured using the method described by Bates et al. [41] and Deuschle et al. [42], respectively. Proline and P5C contents in the eluate were quantified using ninhydrin assay and the *o*-aminobenzaldehyde method, respectively.

2.6. RNA Isolation and Expression Quantification

Fresh leaves (200 mg) were mixed with RNAiso Plus reagent (Takara, Nojihigashi 7-4-38 Kusatsu, Shiga, Japan) for total RNA isolation. First-strand complementary DNA (cDNA) was synthesized with a GoScript Reverse Transcription System (Takara). RT-qPCR reactions were carried out on a BioRad CFX96 qPCR System using the TB Green Premix Ex Taq (Takara). Three biological replications were carried out for each treatment, each with two technical replicates. The relative expression levels of were normalized to actin and calculated using the $2^{-\Delta\Delta C_t}$ method [43]. Supplementary Table S1 provides the gene-specific primer used for qRT-PCR.

2.7. Statistical Analysis

All measurements were performed with three replicates per treatment. The experimental results are presented as mean \pm SE. Duncan's multiple range test was performed to compare the means of separate replicates. Statistical significance was established at $p < 0.05$. Statistical analysis of all measurements was performed using SAS 9.1.3 software (SAS Institute Inc., Cary, NC, USA). Heatmap and Pearson correlation analyses were conducted using MetaboAnalyst 4.0 (<http://www.metaboanalyst.ca>, assessed on 20 September 2021).

3. Results

3.1. Leaf Water Potential, Chlorophyll Content, and Lipid Peroxidation Level

Drought and Exo-H₂O₂ treatments for 10 days significantly decreased the leaf water potential (Ψ_w) (Table 1). The drought-responsive decrease in Ψ_w was earlier and higher than that observed in Exo-H₂O₂ treatment. The chlorophyll content on day 10 also tended to decrease in both drought and Exo-H₂O₂ treatments compared to the control (Table 1). The concentration of MDA, as a marker of lipid peroxidation caused by oxidative stress, significantly increased to 2.0- and 1.3-fold in drought and Exo-H₂O₂ treatments, respectively, compared to the control on day 10 (Table 1).

Table 1. The changes in leaf water potential (Ψ_w), chlorophyll content, and lipid peroxidation level under control, exogenous H₂O₂ (Exo-H₂O₂), or drought treatments for 10 days.

	Days after Treatment		
	0	5	10
	Leaf water potential (Ψ_w , MPa)		
Control	-0.44 ± 0.02^a	-0.44 ± 0.02^a	-0.48 ± 0.02^a
Drought		-0.66 ± 0.03^b	-1.20 ± 0.02^d
Exo-H ₂ O ₂		-0.47 ± 0.02^a	-1.07 ± 0.04^c
	Chlorophyll (mg g ⁻¹ FW)		
Control	1.61 ± 0.08^{ab}	1.73 ± 0.10^a	1.62 ± 0.09^{ab}
Drought		1.45 ± 0.07^{abc}	1.22 ± 0.06^c
Exo-H ₂ O ₂		1.63 ± 0.09^{ab}	1.34 ± 0.05^{bc}
	Lipid peroxidation (MDA, nmol g ⁻¹ FW)		
Control	4.55 ± 0.24^d	4.46 ± 0.32^d	4.84 ± 0.23^{cd}
Drought		5.85 ± 0.24^{bc}	9.45 ± 0.33^a
Exo-H ₂ O ₂		4.80 ± 0.35^{cd}	6.33 ± 0.43^b

Results are represented as mean \pm SE for $n = 3$. Different letters in a vertical column or a horizontal row indicate values that are significantly different at $p < 0.05$ according to Duncan's multiple range test.

3.2. ROS Status and Antioxidative Enzymes Activity

To quantify the oxidative responses of plants to drought or Exo-H₂O₂ treatment, we determined the O₂^{•-} and H₂O₂ contents and enzyme activities of POX, SOD, and CAT. The O₂^{•-} concentration significantly increased in both the treatments throughout the experimental period (except on day 5 of Exo-H₂O₂ treatment). On day 10, the accumulation of O₂^{•-} was much higher in drought treatment as it showed a 5.2-fold increase, while Exo-H₂O₂ treatment showed a 2.4-fold increase when compared to the control on day 0

(40.6 pmol g⁻¹ FW) (Figure 1A). A significant increase in H₂O₂ concentration and accumulation was also observed in both treatments. Drought-responsive H₂O₂ accumulation was higher than that in Exo-H₂O₂ treatment (Figure 1B). The enzymatic activity of cell wall POX also increased in both the treatments. The activation of POX in both drought and Exo-H₂O₂ treatments was not significant on day 5, whereas it was 1.4-fold higher in drought treatment than that in Exo-H₂O₂ treatment on day 10 (Figure 1C). The activity of SOD progressively increased with time in both the treatments. The SOD activity on day 10 was 46.2 and 33.8 unit mg⁻¹ protein in drought and Exo-H₂O₂ treatments, respectively (Figure 1D). The CAT activity was not significantly different between treatments throughout the experimental period (Figure 1E). These results indicated that the endogenous H₂O₂ level affects the ROS status and activities of antioxidant enzymes.

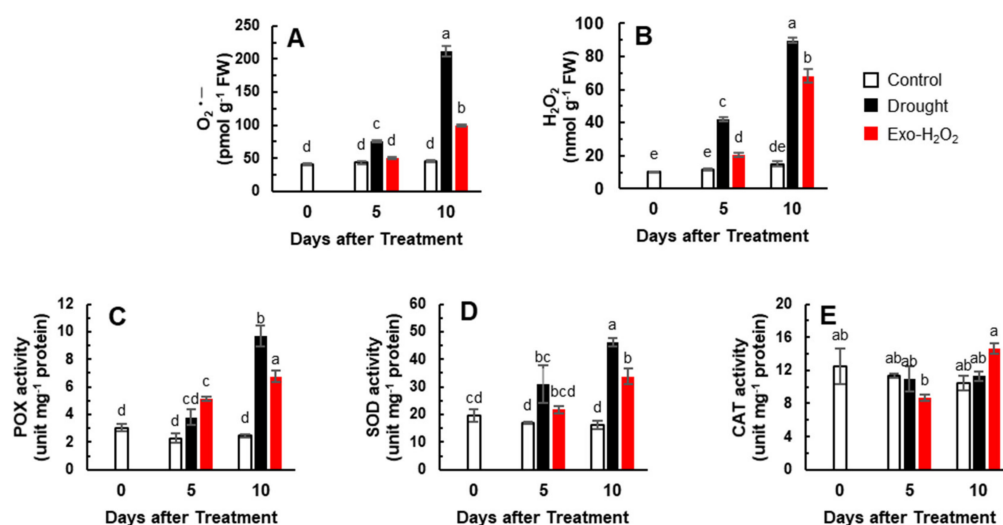


Figure 1. Changes in the concentration of ROS and in the activity of antioxidative enzymes in the leaves of control, drought-, or exogenous H₂O₂ (Exo-H₂O₂) -treated plants for 10 days. (A) O₂^{•-} and (B) H₂O₂ concentration, (C) peroxidase (POX), (D) superoxide dismutase (SOD), and (E) catalase (CAT) activity. Results are represented as mean ± SE for n = 3. Different letters indicate values that are significantly different at p < 0.05 according to Duncan's multiple range test.

3.3. Endogenous ABA and SA Status, and ABA and SA Synthesis and Signaling Genes Expression

In order to effects of drought or Exo-H₂O₂ treatment on phytohormone metabolism, ABA and SA contents and their synthesis- and signaling-related gene expressions were measured. Endogenous ABA level on day 5 was significantly increased only in drought-treated leaves. The accumulation of ABA occurred in both treatments, with 22- and 6.4-fold increase in drought and Exo-H₂O₂ treatments, respectively, compared to the control on day 0 (Table 2). Levels of SA were significantly higher on day 5, then decreased on day 10 in both treatments. The highest SA level was recorded on day 5 in the Exo-H₂O₂ treatment, with a 1.9-fold higher level than that measured in the drought treatment (Table 2). The resulting ratio of ABA/SA on day 10 was 27.55 and 6.12 in drought and Exo-H₂O₂ treatments, respectively (Table 2).

The expression of the ABA synthesis-related gene, *9-cis-epoxycarotenoid dioxygenase* (*NCED3*), was enhanced from day 5 (e.g., 4.2- and 2.3-fold in drought and Exo-H₂O₂ treatments, respectively) and continued until day 10. The enhancement of *NCED3* was much higher in the drought treatment (7.6-fold) (Figure 2A). The expressions of the ABA receptor gene (*PYL1*) and ABA signaling gene (*MYC2*) were also highly enhanced in the drought treatment compared to that in Exo-H₂O₂ treatment throughout the experimental period (Figure 2B,C). Higher expression of the SA synthesis gene, *iso-chorismate synthase 1* (*ICS1*), was observed in both drought (4.6-fold) and Exo-H₂O₂ treatments (5.1-fold) on day 5, which then decreased up until 10 days, but the expression of *ICS1* was significantly

higher in Exo-H₂O₂ than in the drought treatment (Figure 2D). The expression of the *non-race-specific-disease resistance 1 gene (NDR1)* on day 5 was significantly higher in drought treatment than in Exo-H₂O₂ treatment, but it reversed on day 10 (Figure 2E). The expression of the SA signaling gene, *non-expressor of pathogenesis-related gene (NPR1)*, followed a similar pattern of endogenous SA level throughout the experimental period (Figure 2F). Therefore, it appears that the SA synthesis- and signaling-related pathway is promoted at a lower endogenous H₂O₂ level, whereas the ABA synthesis- and signaling-related pathway is enhanced at a higher endogenous H₂O₂ level.

Table 2. The changes in levels of endogenous abscisic acid (ABA) and salicylic acid (SA), and in the ratio of ABA to SA under control, drought, or exogenous H₂O₂ (Exo-H₂O₂) treatments for 10 days.

	Days after Treatment		
	0	5	10
ABA (ng g ⁻¹ FW)			
Control	5.24 ± 0.29 ^c	6.44 ± 0.36 ^c	5.93 ± 0.11 ^c
Drought		32.66 ± 0.04 ^b	115.09 ± 5.56 ^a
Exo-H ₂ O ₂		7.24 ± 0.14 ^c	33.45 ± 0.34 ^b
SA (ng g ⁻¹ FW)			
Control	2.21 ± 0.20 ^f	2.69 ± 0.36 ^{ef}	3.21 ± 0.11 ^e
Drought		7.09 ± 0.13 ^b	4.18 ± 0.19 ^d
Exo-H ₂ O ₂		13.45 ± 0.37 ^a	5.49 ± 0.24 ^c
ABA/SA ratio			
Control	2.40 ± 0.13 ^d	2.48 ± 0.20 ^d	1.85 ± 0.03 ^d
Drought		4.61 ± 0.08 ^c	27.55 ± 0.74 ^a
Exo-H ₂ O ₂		0.54 ± 0.01 ^e	6.12 ± 0.23 ^b

Results are represented as mean ± SE for *n* = 3. Different letters in a vertical column or a horizontal row indicate values that are significantly different at *p* < 0.05 according to Duncan's multiple range test.

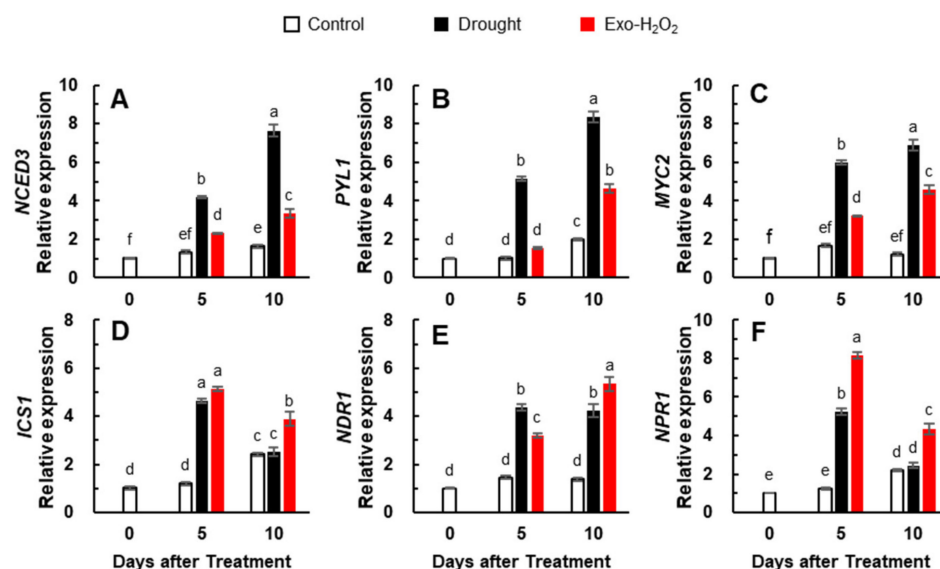


Figure 2. Changes in the expression of (A) ABA synthesis-related gene *NCED3*, (B) ABA receptor gene *PYL1*, (C) ABA signaling-related gene *MYC2*, (D) SA synthesis-related gene *ICS1*, (E) *NDR1*, and (F) SA signaling-related gene *NPR1* in the leaves of control, drought-, or exogenous H₂O₂ (Exo-H₂O₂)-treated plants for 10 days. Results are represented as mean ± SE for *n* = 3. Different letters indicate values that are significantly different at *p* < 0.05 according to Duncan's multiple range test.

3.4. Production of ROS and Expression of ROS Signaling Genes

The expression of *NADPH oxidase*-encoding gene was significantly upregulated only in the drought treatment (5.1-fold) on day 5, but then was continuously enhanced in both

treatments. The enhancement was much higher in drought treatment on day 10, as shown by a 10.2- and 4.4-fold increase in the drought and Exo-H₂O₂ treatments, respectively (Figure 3A). One of the ROS-responsive signaling genes, *MAPK6*, was significantly enhanced only in the drought treatment (3.2-fold) on day 5, and highly enhanced in both treatments on day 10 (9.8- and 5.0-fold in drought and Exo-H₂O₂ treatments, respectively) (Figure 3B). The expression of *OXI1* showed responses similar to those of *MAPK6*, representing a 8.1- and 5.9-fold higher expression in drought and Exo-H₂O₂ treatments, respectively, on day 10 (Figure 3C).

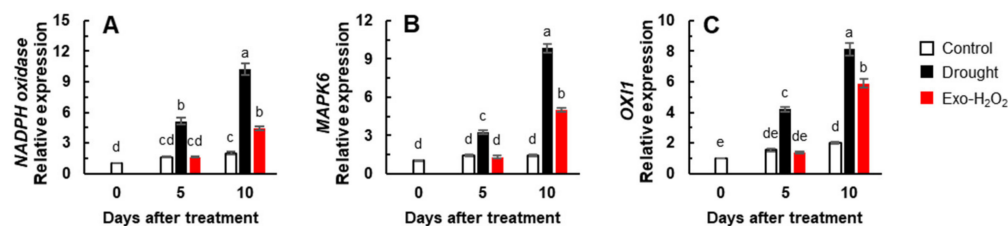


Figure 3. Changes in the expression of (A) *NADPH oxidase*, (B) transcription factor *MAPK6*, and (C) *oxidative signal-inducible (OXI1)* gene in the leaves of control, drought-, or exogenous H₂O₂ (Exo-H₂O₂)-treated plants for 10 days. Results are represented as mean \pm SE for $n = 3$. Different letters indicate values that are significantly different at $p < 0.05$ according to Duncan's multiple range test.

3.5. Proline and P5C Concentration, and Proline Metabolism-Related Gene Expression

To evaluate the effects of altered H₂O₂ levels on proline metabolism, P5C and proline concentrations and proline metabolism-related gene expression were evaluated. Drought Exo-H₂O₂ treatments showed a progressive increase in P5C concentration. Drought-responsive enhancement of P5C was significantly higher than Exo-H₂O₂-responsive enhancement, as shown by 5.8- and 2.4-fold increased levels after 10 days in drought and Exo-H₂O₂ treatments, respectively, compared to the control (Figure 4A). The increase in proline concentration and its accumulation was also significant in both the treatments. The increase in proline concentration was much higher in drought treatment than in Exo-H₂O₂ treatment, with a 14.1- and 2.7-fold increase on day 10 in drought and Exo-H₂O₂ treatments, respectively, compared to the control on day 0 (Figure 4B). The resulting ratio of proline/P5C on day 10 was 3.9 and 1.8 in drought and Exo-H₂O₂ treatments, respectively.

The expression of P5CS-encoding genes (*P5CS1* and *P5CS2*) enhanced in a pattern with a much higher expression in drought treatment during the first 5 days and then a significant decrease in both treatments on day 10 (Figure 4C,D). The expression of P5C reductase-encoding gene (*P5CR*) enhanced to 4.4- and 3.3-fold in drought and Exo-H₂O₂ treatments, respectively, on day 5. The *P5CR* expression in drought continued to enhance (7.7-fold), while it remained restricted in Exo-H₂O₂ (2.2-fold) treatment (Figure 4E). The expression of *ProDH* reduced in both treatments on day 5, while it was enhanced strongly in drought (6.4-fold) and slightly in Exo-H₂O₂ (2.4-fold) treatments on day 10 (Figure 4F). The expression of the P5C dehydrogenase-encoding gene (*P5CDH*) was continuously reduced along with the progression of drought, whereas it was remarkably enhanced on 10 days after Exo-H₂O₂ treatment (Figure 4G). Thus, drought-induced H₂O₂ leads to high upregulation of P5CR and ProDH expression, resulting in increase of the proline/P5C ratio, compared to Exo-H₂O₂ treatment.

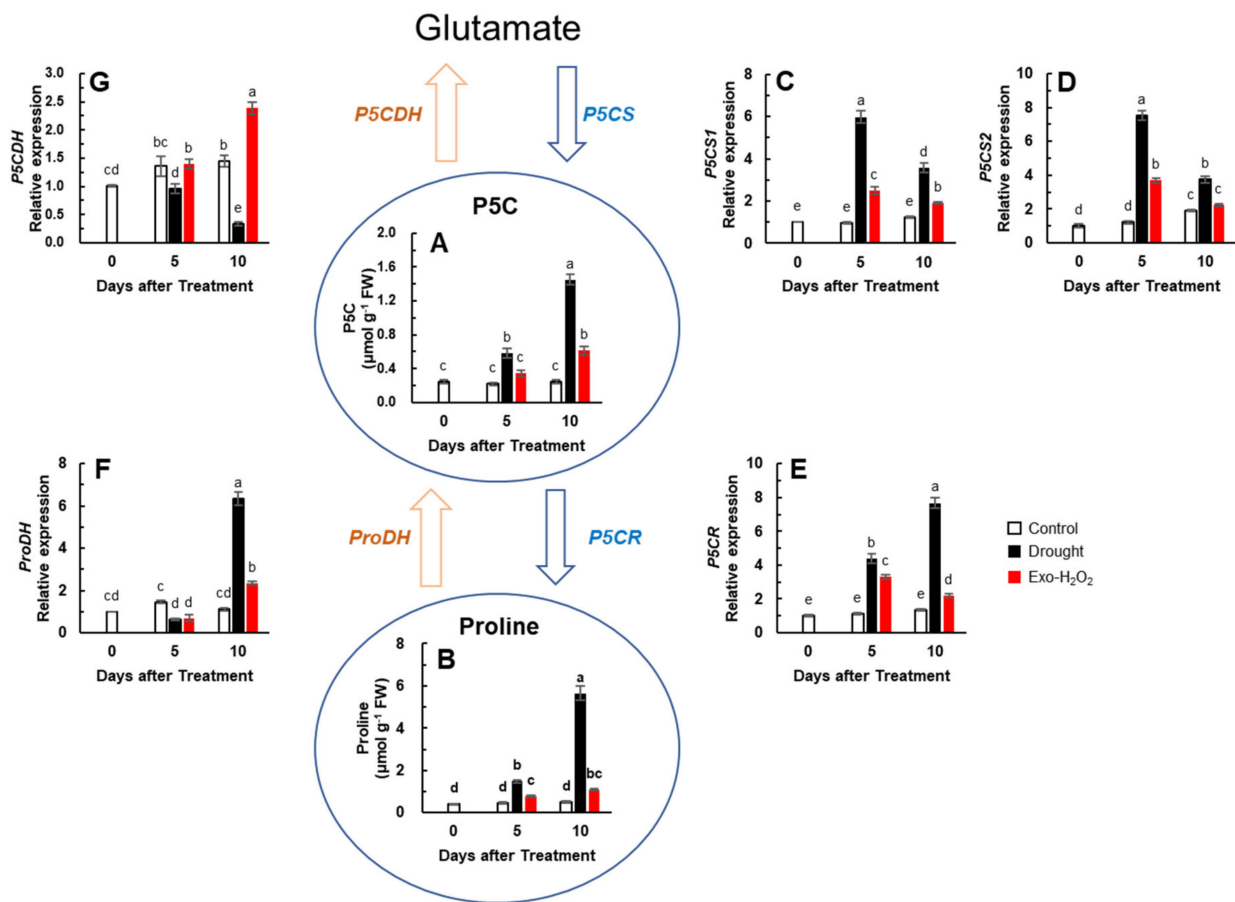


Figure 4. Changes in proline metabolism in the leaves of control, drought-, or exogenous H_2O_2 (Exo- H_2O_2)-treated plants for 10 days. (A) Pyrroline-5-carboxylate (P5C) and (B) proline content, and expression of (C) *P5C synthase 1* (*P5CS1*), (D) *P5CS2*, (E) *P5C reductase* (*P5CR*), (F) *proline dehydrogenase* (*ProDH*), and (G) *P5C dehydrogenase* (*P5CDH*). Results are represented as mean \pm SE for $n = 3$. Different letters indicate values that are significantly different at $p < 0.05$ according to Duncan's multiple range test.

3.6. Heatmap Visualization and Pearson Correlation Analysis among the Metabolites or Gene Expression

To further examine the functional implications and correlations of the measured metabolites and gene expression levels in drought and Exo- H_2O_2 treatments, a heatmap and Pearson's correlation coefficients were adapted (Figure 5). Drought had a more positive influence on ABA, ROS, P5C, and proline levels, as well as on the ABA/SA ratio, when compared with that of Exo- H_2O_2 (Figure 5A). Altered ROS level, which positively regulated the expression of *MAPK6* and *OXII*, was closely correlated with ABA and the ABA/SA ratio. The close relationships between ROS and ABA were also found to be positively correlated with P5C and proline, which had a strong correlation with *P5CR* and *ProDH*, as well as with ABA-regulated genes (*NCED3*, *PYL1*, and *MYC2*) (Figure 5B).

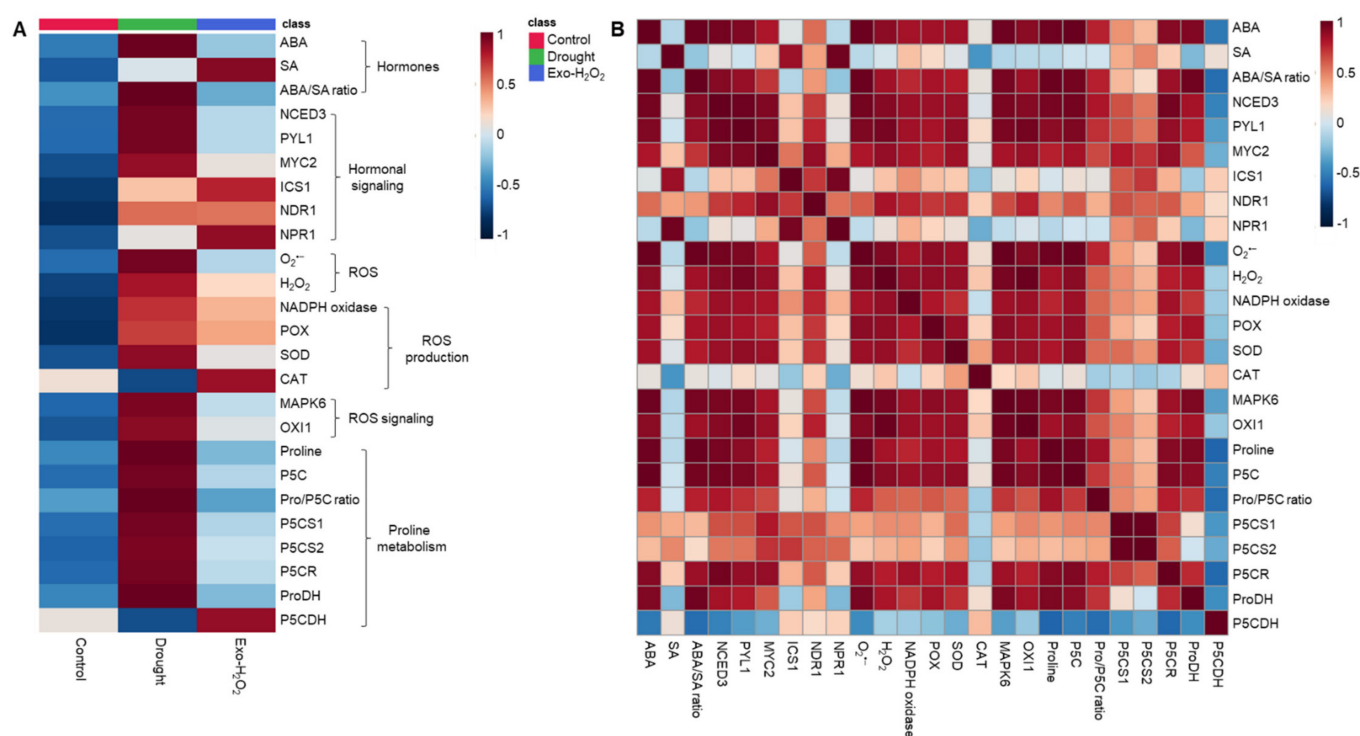


Figure 5. Heatmap analysis of the treatment effect and correlations among the variables measured for 10 days. (A) Heatmap comparing the changes of the identified metabolites or gene expression levels in the leaves of control, drought-, or exogenous H₂O₂ (Exo-H₂O₂)-treated plants for 10 days. The normalization procedure consisted of mean row centering with color scales. (B) Heatmap showing the correlations among the identified metabolites or gene expression levels. Correlation coefficients were calculated based on Pearson's correlation. Red indicates a positive effect, whereas blue indicates a negative effect. Color intensity is proportional to the correlation coefficients.

4. Discussion

4.1. ROS and Hormone Responses to Drought-Induced H₂O₂ and Exogenous H₂O₂

Droughts reduce leaf water potential, which is used as an index of the water status [3,35]. In the present study, a significant decrease of leaf water potential was observed in drought-stressed plants, accompanied by the loss of chlorophyll and enhanced lipid peroxidation level (Table 1). The accumulation of O₂^{•-} and H₂O₂, an early response to various stress stimuli [6,20], occurred in both drought and Exo-H₂O₂ treatments. The endogenous H₂O₂ levels in Exo-H₂O₂ (68.2 nmol g⁻¹ FW) on day 10 corresponded to that of 76% of drought treatment (Figure 1B), which is similar to the results obtained on day 5 of drought treatment in a previous study [6]. During the first 5 days of treatments, the increase in H₂O₂ concentration was concomitant with the enhanced SOD activity (Figure 1D) and *NADPH oxidase* expression (Figure 3A) in drought treatment and with POX activity in Exo-H₂O₂ treatment (Figure 1C). Wang et al. [44] reported that endogenous H₂O₂ accumulation in the apoplast was triggered by both cell wall peroxidase and membrane-linked *NADPH oxidase*. It has been documented that SA is involved in the production of H₂O₂, leading to SA-induced abiotic and biotic stress resistance [20,45]. In the present study, during the first 5 days when the increase in SA levels was predominant, the increased endogenous H₂O₂ level coincided with the increased activation of SA-dependent POX in the Exo-H₂O₂ treatment, and was mainly due to ABA- and/or SA-dependent SOD activity and *NADPH oxidase* expression in the drought treatment (Table 2, Figures 1C,D and 3A), in accordance with SA-mediated H₂O₂ production by activating membrane-linked *NADPH oxidase* [46] and cell wall peroxidase [44,47]. During the latter 5 days, when ABA accumulation with an antagonistic depression of SA was remarked, the accumulation of H₂O₂ occurred with a proportional enhancement of POX and SOD activity and *NADPH oxidase* expression in an

ABA-dependent manner (Table 2, Figures 1C,D and 3A). Ample evidence has shown that H₂O₂ generated by SA-mediated POX and NADPH oxidases acts downstream of ABA signaling in mediating drought-induced stress responses [47–50]. Our recent study reported that SA-stimulated H₂O₂ accumulation and SA responses during the early drought phase are part of upstream H₂O₂-stimulated ABA accumulation, which causes ABA signaling and responses, leading to severe drought symptoms during the late phase [6]. The present data indicate that during the first 5 days, H₂O₂ is produced mainly from SA-mediated activation of NADPH oxidase in drought treatment and POX in the Exo-H₂O₂ treatment, whereas ROS accumulation at day 10 was due to the increase in SOD activity (an H₂O₂-producing enzyme), and in NADPH induction (superoxide-producing enzyme), respectively, in an ABA-dependent manner.

4.2. H₂O₂-Responsive Interaction between ROS and Hormonal Signaling

The altered endogenous H₂O₂ level was strongly correlated ($p < 0.001$) to the expression of two protein kinases (*MAPK6* and *OX11*), which are an essential part of the signal transduction pathway linking oxidative burst signaling to diverse downstream responses [2,13,34,51]. MAPKs, which are downstream of *OX11* [13], are known to be involved in H₂O₂ signaling ability for regulating hormonal and metabolic responses [6,22,29,50]. With respect to ROS signaling, a preponderance of evidence supports ABA as a key regulator of stress responses [5,6,34]. Indeed, in the present study, the endogenous ABA level (Table 2) and the expression of *NCED3* and *MYC2* (Figure 2A,C) in drought treatment were consistent with a progressive increase in the endogenous H₂O₂ level, leading to a proportional upregulation of *MAPK6* (Figure 3B) and *OX11* (Figure 3C), while the expression of these genes was not significantly activated in Exo-H₂O₂ treatment during the first 5 days when the ABA level did not change significantly (Figure 3). Moreover, the overall pattern of *MAPK6* and *OX11* (Figure 3B,C) indicated that they are ROS level-responsive (Figure 1A,B) ABA-regulated genes (Figure 2A–C), in accordance with our previous results obtained from a time course of drought intensity [6]. Similarly, in Arabidopsis, overexpression of AtMPK6 enhanced the ABA-dependent H₂O₂ production, which is blocked in the *mpk6* mutant [52,53]. In addition, the inhibition of MAPK signaling by PD98059 decreases sensitivity to the response of ABA under drought conditions [54]. The endogenous SA level and the expression of SA-related genes (*ICS1* and *NPR1*) in drought treatment (Figure 2D,F) progressively decreased with an antagonistic increase in the ABA level (Table 2) and ABA-related gene expression (Figure 2A–C), along with ROS accumulation (Figure 1A,B). The SA-signaling genes (*NDR1* and *NPR1*) were highly developed in Exo-H₂O₂ on day 5 (Figure 2E,F), in which the endogenous H₂O₂ level was relatively lower (≤ 20 nmol g⁻¹ FW) (Figure 1B). These enhanced SA-signaling genes did not significantly activate *MAPK6* and *OX11* (Figure 3B,C). The time-course analysis showed that the crosstalk between H₂O₂ and SA has a much earlier peak than in ABA [6,55]. In the present study, an altered endogenous H₂O₂ level was highly correlated with increased ABA and ABA-regulated genes, but not with SA responses (Figure 5B). Therefore, a positive feedback loop between H₂O₂- and ABA-mediated pathways might lead to upregulation of *MAPK6* via *OX11*, thereby activating ABA synthesis and signaling genes (*NCED3* and *MYC2*). Thus, the actions of this core pathway in the control of proline metabolism under drought stress needs to be discussed further.

4.3. H₂O₂-Responsive Hormonal Regulation of Proline Metabolism

Along with ROS accumulation, proline is the most common free amino acid to accumulate in the plants exposed to drought stress [5,30,35,56]. Based on the data obtained during the entire experimental period, the correlation between endogenous H₂O₂ level, P5C, and proline concentration was highly positive, and these parameters were also positively correlated with ROS- and ABA-signaling genes' expression (Figure 5B). Indeed, it has been documented that H₂O₂ causes proline accumulation or promotes ABA-induced proline accumulation [23,57]. Previous results reveal that H₂O₂ produced by NADPH

oxidase increases proline accumulation under drought or osmotic stress [5,27], with a strong correlation with ABA accumulation [34,56]. However, in the present study, the data collected in Exo-H₂O₂, especially during the first 5 days, did not directly match these linear relationships. For instance, the enhanced H₂O₂ level in Exo-H₂O₂ treatment led to a significant increase in P5C and proline levels (Figure 4A,B), although the ABA level and *NADPH oxidase* gene expression did not change during the first 5 days (Table 2, Figure 3A). The Exo-H₂O₂-responsive increases in P5C and proline levels were found to be associated with SA-dependent proline synthesis-related genes (Figure 4C–E), possibly related to SA-mediated activation of POX and not with the NADPH oxidase-dependent process (Figure 1C). Apart from these early responses to Exo-H₂O₂, the enhanced P5C and proline levels and their accumulation under drought stress were found to be parallel with upregulated *NADPH oxidase* (Figure 3A) in an ABA-related pattern, with an increasing endogenous-H₂O₂ concentration (Figure 1B). These results clearly indicate that drought-induced H₂O₂ (often considered the internal H₂O₂ trigger) might be directly involved in triggering the NADPH oxidase-dependent proline synthesis, but not in Exo-H₂O₂. In drought treatment, P5C and proline levels increased (Figure 4A,B) along with H₂O₂ accumulation, with proportional enhancements of ROS-signaling genes (*OXI1* and *MAPK6*) (Figure 3B,C) and ABA-regulated genes (*NCED3*, *PYL1*, and *MYC2*) (Figure 2A–C), suggesting a greater ABA-dependent proline accumulation in higher H₂O₂ level. This observation further indicates that higher proline accumulation does not directly contribute to the scavenging of cellular ROS, although studies show that proline metabolism has a function as ROS scavenger [30]. The proline levels in plant cells depend on tight regulation of its biosynthesis and degradation catabolism. Proline accumulation under stress is accompanied by the upregulation of proline biosynthesis (*P5CS* and *P5CR*) and downregulation of proline catabolism-related genes (*ProDH* and *P5CDH*) [5,6,33,35], in an ABA-dependent manner [31,34]. Indeed, in drought treatment, P5C and proline accumulation occurred with highly enhanced expression of *P5CS1*, *P5CS2*, and *P5CR* (Figure 4C–E), accompanied with a progressive enhancement of *NADPH oxidase* (Figure 3A), which coincided with the enhanced H₂O₂-responsive increases in ABA level (Table 2) and ABA-regulated genes' expressions (Figure 2A–C). This observation confirmed the given hypothesis that H₂O₂ generated by NADPH oxidases acts downstream of ABA signaling [48,49,58], and involves in proline accumulation by upregulating *P5CS* [27]. However, in Exo-H₂O₂ treatment, the pattern of P5C and proline was not directly associated with those of H₂O₂- and ABA-mediated NADPH oxidase, as shown lower activation of *P5CS*, *P5CR* (Figure 4C–E), and *NADPH oxidase* (Figure 3A), even though endogenous H₂O₂ was enhanced up to 68.2 nmol g⁻¹ FW on day 10 (Figure 1B). Besides the interaction between H₂O₂- and ABA-signaling in proline biosynthesis, it was noteworthy that significant enhancements of *P5CS* and *P5CR* also coincided with the increased SA level and upregulation of SA-related genes (Figure 2D–F), especially when endogenous H₂O₂ was less than 42 nmol g⁻¹ FW (e.g., during the first 5 days after both treatments). This observation suggests that SA signaling is also involved in the activation of proline synthesis as part of early stress response, confirming the role of SA as a signal of different types of stresses [20,45,59]. In our previous studies, leaf spraying with 30 mL of 0.5 mM SA enhanced enzymatic activity of SOD and their encoding genes, and induced proline accumulation with enhanced synthesis-related genes (*P5CS* and *P5CR*) [5].

Proline is oxidized to glutamate by the sequential action of ProDH and P5CDH [30,60]. In the present study, the expression of *ProDH* tended to decrease with increasing endogenous proline levels, except in the data of 10 days after drought treatment (Figure 4B,F). The enhanced activity of ProDH leads to ROS formation in mitochondria by coupling proline oxidation to reduction of the respiratory electron transport chain [30,57]. Indeed, the highest activation of *ProDH* (on 10 days after drought treatment) coincided with the most accumulated proline and ROS level in an ABA-dependent manner (Figures 1B and 4B,F). Mani et al. [60] reported that altered levels of *ProDH* cause hypersensitivity to proline and its analog. Moreover, an exceptional enhancement of *P5CDH*, the second enzyme for

proline catabolism, was observed on day 10 following Exo-H₂O₂ treatment, which showed a considerable accumulation (68.2 nmol g⁻¹ FW) of endogenous H₂O₂ (Figure 1B). Thus, an overexpression of *ProDH* and *P5CDH* might be part of the hypertensive response to over-produce H₂O₂ and/or proline, predicting an increase in proline-P5C cycling, leading to ROS accumulation [25,57,61].

5. Conclusions

The present data indicate that hormonal interaction with proline metabolism is governed by endogenous levels of ROS (especially H₂O₂), as shown by SA-mediated activation of proline synthesis at lower endogenous H₂O₂ levels, and a predominant ABA-dependent proline accumulation along with ROS accumulation. Furthermore, to the best of our knowledge, the present data are the first to report that H₂O₂-responsive SA and ABA involves in ROS signaling and proline metabolism in rapeseed leaves (Figure 6), representing two distinct phases characterized by the following: (1) an active NDR1-mediated SA-dependent proline synthesis with upregulation of *P5CS* and *P5CR*, and depression of *ProDH* as an acclamatory process at lower level of endogenous H₂O₂ produced by either Exo-H₂O₂ or drought treatment; and (2) drought-induced proline accumulation with ABA-dependent MAPK6 activation via *OXI1*, leading to upregulation of *ProDH* as hypersensitive responses to a higher H₂O₂ level. Future studies are necessary (1) to define the threshold at which proline level switches from inducing cellular protection to hypersensitivity to over-produced ROS and/or proline, and (2) to elucidate hormonal interaction with proline in redox regulation.

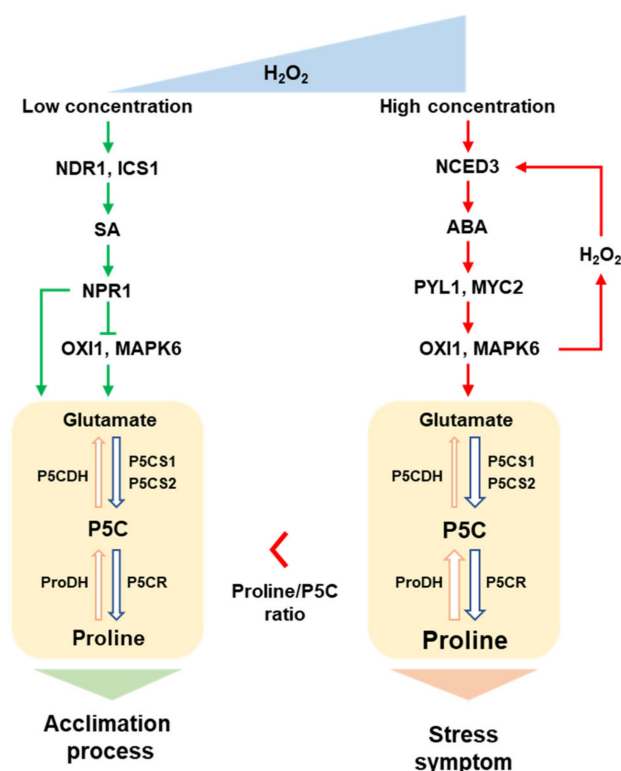


Figure 6. Proposed model of crosstalk between ROS signaling, hormones, and proline metabolism in response to endogenous H₂O₂ level. Green and red arrows represent the SA- and ABA-dependent pathways, respectively.

Supplementary Materials: The following supporting information can be downloaded at: <https://www.mdpi.com/article/10.3390/antiox11030566/s1>, Supplementary Table S1: Primer sequences used for qRT-PCR analysis.

Author Contributions: Conceptualization, B.-R.L., V.H.L. and T.-H.K.; methodology, B.-R.L., V.H.L. and T.-H.K.; formal analysis B.-R.L., V.H.L., S.-H.P., M.A.M. and D.-W.B.; investigation, B.-R.L., V.H.L. and T.-H.K.; writing—original draft preparation, B.-R.L., V.H.L. and T.-H.K.; review and editing, B.-R.L., V.H.L., S.-H.P., M.A.M., D.-W.B. and T.-H.K.; supervision, T.-H.K.; project administration, T.-H.K.; funding acquisition, T.-H.K. All authors have read and agreed to the published version of the manuscript.

Funding: This work was supported by a grant from the National Research Foundation of South Korea under project NRF-2021R1A4A1031220.

Institutional Review Board Statement: Not applicable.

Informed Consent Statement: Not applicable.

Data Availability Statement: Data is contained within the article and its Supplementary Materials.

Conflicts of Interest: The authors declare no conflict of interest.

References

1. Smirnov, N. The role of active oxygen in the response of plants to water deficit and desiccation. *New Phytol.* **1993**, *125*, 27–58. [[CrossRef](#)] [[PubMed](#)]
2. Mittler, R.; Vanderauwera, S.; Gollery, M.; Breusegem, F.V. Reactive oxygen gene network of plants. *Trends Plant Sci.* **2004**, *9*, 490–498. [[CrossRef](#)] [[PubMed](#)]
3. Lee, B.R.; Kim, K.Y.; Jung, W.J.; Avice, J.C.; Ourry, A.; Kim, T.H. Peroxidases and lignification in relation to the intensity of water-deficit stress in white clover (*Trifolium repens* L.). *J. Exp. Bot.* **2007**, *58*, 1271–1279. [[CrossRef](#)] [[PubMed](#)]
4. Miller, G.; Suzuki, N.; Ciftci-Yilmaz, S.; Mittler, R. Reactive oxygen species homeostasis and signalling during drought and salinity stresses. *Plant Cell Environ.* **2010**, *33*, 453–467. [[CrossRef](#)]
5. La, V.H.; Lee, B.R.; Islam, M.T.; Park, S.H.; Jung, H.I.; Bae, D.W.; Kim, T.H. Characterization of salicylic acid-mediated modulation of the drought stress responses: Reactive oxygen species, proline, and redox state in *Brassica napus*. *Environ. Exp. Bot.* **2019**, *157*, 1–10. [[CrossRef](#)]
6. Park, S.H.; Lee, B.R.; La, V.H.; Mamun, M.A.; Bae, D.W.; Kim, T.H. Characterization of salicylic acid- and abscisic acid-mediated photosynthesis, Ca²⁺ and H₂O₂ accumulation in two distinct phases of drought stress intensity in *Brassica napus*. *Environ. Exp. Bot.* **2021**, *186*, 104434. [[CrossRef](#)]
7. Caruso, C.; Chilosi, G.; Caporale, C.; Leonardi, L.; Bertini, L.; Magro, P.; Buonocore, V. Induction of pathogenesis-related proteins in germinating wheat seeds infected with *Fusarium culmorum*. *Plant. Sci.* **1999**, *140*, 107–120. [[CrossRef](#)]
8. Islam, M.T.; Lee, B.R.; Park, S.H.; La, V.H.; Jung, W.J.; Bae, D.W.; Kim, T.H. Hormonal regulations in soluble and cell-wall bound phenolic accumulation in two cultivars of *Brassica napus* contrasting susceptibility to *Xanthomonas campestris* pv. *campestris*. *Plant Sci.* **2019**, *285*, 132–140. [[CrossRef](#)]
9. Mamun, M.A.; Islam, M.T.; Lee, B.R.; La, V.H.; Bae, D.W.; Kim, T.H. Genotypic variation in resistance gene-mediated calcium signaling and hormonal signaling involved in effector-triggered immunity or disease susceptibility in the *Xanthomonas campestris* pv. *Campestris*-*Brassica napus*. *Plants* **2020**, *9*, 303. [[CrossRef](#)]
10. Mittler, R. Oxidative stress, antioxidants and stress tolerance. *Trends Plant Sci.* **2002**, *7*, 405–410. [[CrossRef](#)]
11. Lee, B.R.; Li, L.S.; Jung, W.J.; Jin, Y.L.; Avice, J.C.; Querry, A.; Kim, T.H. Water deficit-induced oxidative stress and the activation of antioxidant enzymes in white clover leaves. *Biol. Plant.* **2009**, *53*, 505–510. [[CrossRef](#)]
12. Foyer, C.H.; Noctor, G. Redox signaling in plants. *Antioxid. Redox Signal.* **2013**, *18*, 2087–2090. [[CrossRef](#)]
13. Rentel, M.C.; Lecourieux, D.; Ouaked, F.; Usher, S.L.; Petersen, L.; Okamoto, H.; Knight, H.; Peck, S.C.; Grierson, C.S.; Hirt, H.; et al. OXI1 kinase is necessary for oxidative burst-mediated signaling in *Arabidopsis*. *Nature* **2004**, *427*, 858–861. [[CrossRef](#)]
14. Baxter, A.; Mittler, R.; Suzuki, N. ROS as key players in plant stress signaling. *J. Exp. Bot.* **2014**, *65*, 1229–1240. [[CrossRef](#)]
15. Choudhury, F.K.; Rivero, R.M.; Blumwald, E.; Mittler, R. Reactive oxygen species, abiotic stress and stress combination. *Plant J.* **2017**, *90*, 856–867. [[CrossRef](#)]
16. Huang, S.; VanAken, O.; Schwarzländer, M.; Belt, K.; Millar, A.H. The roles of mitochondrial reactive oxygen species in cellular signaling and stress responses in plants. *Plant Physiol.* **2016**, *171*, 1551–1559. [[CrossRef](#)]
17. Foyer, C.H. Reactive oxygen species, oxidative signaling and the regulation of photosynthesis. *Environ. Exp. Bot.* **2018**, *154*, 134–142. [[CrossRef](#)]
18. Hasanuzzaman, M.; Bhuyan, N.H.M.B.; Zulfiqar, F.; Raza, A.L.; Mohsin, S.M.; Mahmud, J.A.; Fujita, M.; Fotopoulos, V. Reactive oxygen species and antioxidant defense in plants under abiotic stress: Revisiting the crucial role of a universal defense regulator. *Antioxidants* **2020**, *9*, 681. [[CrossRef](#)]
19. Pandey, P.; Singh, J.; Achary, V.M.M.; Reddy, M.K. Redox homeostasis via gene families of ascorbate-glutathione pathway. *Front. Plant Sci.* **2015**, *3*, 25. [[CrossRef](#)]
20. Raja, V.; Majeed, U.; Kang, H.; Andrabi, K.I.; John, R. Abiotic stress: Interplay between ROS, hormones and MAPKs. *Environ. Exp. Bot.* **2017**, *137*, 142–157. [[CrossRef](#)]

21. Willems, P.; Mhamdi, A.; Stael, S.; Storme, V.; Kerchev, P.; Noctor, G.; Gevaert, K.; Breusegem, F.V. The ROS wheel: Refining ROS transcriptional foot prints in Arabidopsis. *Plant Physiol.* **2016**, *171*, 1720–1733. [[CrossRef](#)]
22. Xia, X.J.; Zhou, Y.H.; Shi, K.; Zhou, J.; Foyer, C.H.; Yu, J.Q. Interplay between reactive oxygen species and hormones in the control of plant development and stress tolerance. *J. Exp. Bot.* **2015**, *66*, 2839–2856. [[CrossRef](#)]
23. Seki, M.; Umezawa, T.; Urano, K.; Shinozaki, K. Regulatory metabolic networks in drought stress responses. *Curr. Opin. Plant Biol.* **2007**, *10*, 296–302. [[CrossRef](#)]
24. Barba-Espin, G.; Diaz-Vivancos, P.; Clemente-Moreno, M.J.; Albacete, A.; Faize, L.; Faize, M.; Pérez-Alfocea, F.; Hernández, J.A. Interaction between hydrogen peroxide and plant hormones during germination and the early growth of pea seedlings. *Plant Cell Environ.* **2010**, *33*, 981–994. [[CrossRef](#)]
25. Szabados, L.; Savoure, A. Proline: A multifunctional amino acid. *Trends Plant Sci.* **2010**, *15*, 89–97. [[CrossRef](#)]
26. Rehman, A.U.; Bashir, F.; Ayaydin, F.; Kóta, Z.; Páli, T.; Vass, I. Proline is a quencher of singlet oxygen and superoxide both in in vitro systems and isolated thylakoids. *Physiol. Plant.* **2021**, *172*, 7–18. [[CrossRef](#)]
27. Rejeb, B.K.; Lefebvre-De Vos, D.; Le Disquet, I.; Leprince, A.S.; Bordenave, M.; Maldinev, R.; Jdey, A.; Abdelly, C.; Savouré, A. Hydrogen peroxide produced by NADPH oxidases increases proline accumulation during salt or mannitol stress in Arabidopsis thaliana. *New Phytol.* **2015**, *208*, 1138–1148. [[CrossRef](#)]
28. Miller, G.; Honig, A.; Stein, H.; Suzuki, N.; Mittler, R.; Zilberstein, A. Unraveling delta1-pyrroline-5-carboxylate-proline cycle in plants by uncoupled expression of proline oxidation enzymes. *J. Biol. Chem.* **2009**, *284*, 26482–26492. [[CrossRef](#)]
29. Chen, J.; Zhang, Y.; Wang, C.; Lü, W.; Jin, J.B.; Hua, X. Proline induces calcium-mediated oxidative burst and salicylic acid signaling. *Amino Acids* **2011**, *40*, 1473–1484. [[CrossRef](#)]
30. Rejeb, K.B.; Abdelly, C.; Savouré, A. How reactive oxygen species and proline face stress together. *Plant Physiol. Biochem.* **2014**, *80*, 278–284. [[CrossRef](#)]
31. La, V.H.; Lee, B.R.; Islam, M.T.; Mamun, M.A.; Park, S.H.; Bae, D.W.; Kim, T.H. Characterization of glutamate-mediated hormonal regulatory pathway of the drought responses in relation to proline metabolism in *Brassica napus* L. *Plants* **2020**, *9*, 512. [[CrossRef](#)] [[PubMed](#)]
32. Chung, J.S.; Zhu, J.K.; Bressan, R.A.; Hasegawa, P.M.; Shi, H. Reactive oxygen species mediate Na⁺-induced SOS1 mRNA stability in Arabidopsis. *Plant J.* **2008**, *53*, 554–565. [[CrossRef](#)] [[PubMed](#)]
33. Yang, Y.; Zhang, Y.; Wei, X.; You, J.; Wang, W.; Lu, J.; Shi, R. Comparative antioxidative responses and proline metabolism in two wheat cultivars under short term lead stress. *Ecotoxicol. Environ. Saf.* **2011**, *74*, 733–740. [[CrossRef](#)] [[PubMed](#)]
34. Verslues, P.E.; Kim, Y.S.; Zhu, J.K. Altered ABA, proline and hydrogen peroxide in an Arabidopsis glutamate:glyoxylate aminotransferase mutant. *Plant Mol. Biol.* **2007**, *64*, 205–217. [[CrossRef](#)]
35. Lee, B.R.; Jin, Y.L.; Avice, J.C.; Cliquet, J.B.; Ourry, A.; Kim, T.H. Increased proline loading to phloem and its effects on nitrogen uptake and assimilation in water-stressed white clover (*Trifolium repens*). *New Phytol.* **2009**, *182*, 654–663. [[CrossRef](#)]
36. Hiscox, J.T.; Israelstam, G.F. A method for the extraction of chlorophyll from leaf tissue without maceration. *Can. J. Bot.* **1979**, *57*, 1332–1334. [[CrossRef](#)]
37. Pan, X.Q.; Welti, R.; Wang, W.M. Quantitative analysis of major plant hormones in crude plant extracts by high-performance liquid chromatography-mass spectrometry. *Nat. Protoc.* **2010**, *5*, 986–992. [[CrossRef](#)]
38. Lee, B.R.; Muneer, S.; Park, S.H.; Zhang, Q.; Kim, T.H. Ammonium-induced proline and sucrose accumulation, and their significance in antioxidative activity and osmotic adjustment. *Acta Physiol. Plant.* **2013**, *35*, 2655–2664. [[CrossRef](#)]
39. Lee, T.M.; Lin, Y.H. Changes in soluble and cell wall-bound peroxidase activities with growth in anoxia-treated rice (*Oryza sativa* L.) coleoptiles and roots. *Plant Sci.* **1995**, *106*, 1–7. [[CrossRef](#)]
40. Lin, C.C.; Kao, C.H. Cell wall peroxidase activity, hydrogen peroxidase level and NaCl-inhibited root growth of rice seedling. *Plant Soil* **2001**, *230*, 135–143. [[CrossRef](#)]
41. Bates, L.S.; Waldren, R.P.; Teare, I.D. Rapid determination of free proline for water-stress studies. *Plant Soil* **1973**, *39*, 205–207. [[CrossRef](#)]
42. Deuschle, K.; Funck, D.; Forlani, G.; Stransky, H.; Biehl, A.; Leister, D.; van der Graaff, E.; Kunze, R.; Frommmer, E.B. The Role of Δ1-Pyrroline-5-Carboxylate Dehydrogenase in proline degradation. *Plant Cell* **2004**, *16*, 3413–3425. [[CrossRef](#)]
43. Livak, J.K.; Schmittgen, T.D. Analysis of relative gene expression data using real-time quantitative PCR and the 2^{-ΔΔC_t} method. *Methods* **2001**, *25*, 402–408. [[CrossRef](#)]
44. Wang, W.; Wnag, X.; Huang, M.; Cai, J.; Zhou, Q.; Dal, T.; Cao, W.; Jiang, D. Hydrogen peroxide and abscisic acid mediate salicylic acid-induced freezing tolerance in wheat. *Front. Plant Sci.* **2018**, *9*, 1137. [[CrossRef](#)]
45. Herrera-Vásquez, A.; Salinas, P.; Holuigue, L. Salicylic acid and reactive oxygen species interplay in the transcriptional control of defense genes expression. *Front. Plant Sci.* **2015**, *6*, 171. [[CrossRef](#)]
46. Kalachova, T.; Iakovenko, O.; Kretinin, S.; Kravets, V. Involvement of phospholipase D and NADPH-oxidase in salicylic acid signaling cascade. *Plant Physiol. Biochem.* **2013**, *66*, 127–133. [[CrossRef](#)]
47. Khokon, A.R.; Okuma, E.; Hossain, M.A.; Munemasa, S.; Uraji, M.; Nakamura, Y.; Mori, I.C.; Murata, Y. Involvement of extracellular oxidative burst in salicylic acid induced stomatal closure in Arabidopsis. *Plant Cell Environ.* **2011**, *34*, 434–443. [[CrossRef](#)]

48. Kwak, J.M.; Mori, I.C.; Pei, Z.M.; Leonhardt, N.; Torres, M.A.; Dangl, J.L.; Bloom, R.E.; Bodde, S.; Jones, J.D.G.; Schroeder, J.I. NADPH oxidase *AtrbohD* and *AtrbohF* genes function in ROS-dependent ABA signaling in *Arabidopsis*. *EMBO J.* **2003**, *22*, 2623–2633. [[CrossRef](#)]
49. Bright, J.; Desikan, R.; Hancock, J.T.; Weir, I.S.; Neill, S.J. ABA induced NO generation and stomatal closure in *Arabidopsis* are dependent on H₂O₂ synthesis. *Plant J.* **2006**, *45*, 113–122. [[CrossRef](#)]
50. Zelicourt, A.D.; Colcombet, J.; Hirt, H. The role of MAPK modules and ABA during abiotic stress signaling. *Trends Plant Sci.* **2016**, *21*, 677–685. [[CrossRef](#)]
51. Jalmi, S.K.; Sinha, A.K. ROS mediated MAPK signaling in abiotic and biotic stress-striking similarities and differences. *Front. Plant Sci.* **2015**, *6*, 769. [[CrossRef](#)] [[PubMed](#)]
52. Xing, Y.; Jia, W.; Zhang, J. AtMKK1 mediates ABA-induced *CAT1* expression and H₂O₂ production via AtMPK6-coupled signaling in *Arabidopsis*. *Plant J.* **2008**, *54*, 440–451. [[CrossRef](#)] [[PubMed](#)]
53. Tsugama, D.; Liu, S.; Takano, T. Drought-induced activation and rehydration-induced inactivation of MPK6 in *Arabidopsis*. *Biochem. Biophys. Res. Commun.* **2012**, *426*, 626–629. [[CrossRef](#)] [[PubMed](#)]
54. Lu, C.; Han, M.-H.; Guevara-Garcia, A.; Fedoroff, N.V. Mitogen-activated protein kinase signaling in postgermination arrest of development by abscisic acid. *Proc. Natl. Acad. Sci. USA* **2002**, *99*, 15812–15817. [[CrossRef](#)]
55. Hieno, A.; Naznin, H.A.; Inaba-Hasegawa, K.; Yokogawa, T.; Hayami, N.; Nomoto, M.; Tada, Y.; Yokogawa, T.; Higuchi-Takeuchi, M.; Hanada, K.; et al. Transcriptome analysis and identification of a transcriptional regulatory network in the response to H₂O₂. *Plant Physiol.* **2019**, *180*, 1629–1646. [[CrossRef](#)]
56. Bhaskara, G.B.; Yang, T.H.; Verslus, P.E. Dynamic proline metabolism: Importance and regulation in water limited environments. *Front. Plant Sci.* **2015**, *6*, 484. [[CrossRef](#)]
57. Liang, X.; Zhang, L.; Natarajan, S.K.; Becker, D.F. Proline mechanism of stress survival. *Antioxid. Redox Signal.* **2013**, *19*, 998–1011. [[CrossRef](#)]
58. Zhang, X.; Zhang, L.; Dong, F.; Gao, J.; Galbraith, D.W.; Song, C.P. Hydrogen peroxide is involved in abscisic acid-induced stomatal closure in *Vicia faba*. *Plant Physiol.* **2001**, *126*, 1438–1448. [[CrossRef](#)]
59. Miura, K.; Tada, Y. Regulation of water, salinity, and cold stress responses by salicylic acid. *Front. Plant Sci.* **2014**, *5*, 4. [[CrossRef](#)]
60. Mani, S.; Van De Cotte, B.; Van Montagu, M.; Verbruggen, N. Altered levels of proline dehydrogenase cause hypersensitivity to proline and its analogs in *Arabidopsis*. *Plant Physiol.* **2002**, *128*, 73–83. [[CrossRef](#)]
61. Rizzi, Y.S.; Monteoliva, M.I.; Fabro, G.; Grosso, C.L.; Laróvere, L.E.; Alvarez, M.E. P5CDH affects the pathways contributing to Pro synthesis after ProDH activation by biotic and abiotic stress conditions. *Front. Plant Sci.* **2015**, *6*, 572. [[CrossRef](#)]